Journal of Materials Chemistry C

COMMUNICATION

View Article Online
View Journal | View Issue

Cite this: J. Mater. Chem. C, 2014, 2, 8012

Received 3rd July 2014
Accepted 13th July 2014

DOI: 10.1039/c4tc01428f

www.rsc.org/MaterialsC

Polyelectrolyte multilayer-assisted fabrication of p-Cu_2S/n-CdS heterostructured thin-film phototransistors†

Ramphal Sharma,‡*[ab] Gangri Cai,‡[bc] Dipak V. Shinde,[b] Supriya A. Patil,[b] Shaheed Shaikh,[a] Anil Vithal Ghule,[b] Rajaram S. Mane[b] and Sung-Hwan Han‡*[b]

We demonstrate meticulous fabrication of p-Cu_2S/n-CdS heterojunction thin films using a facile wet-chemical approach. Ion exchange of Cu^+ with Cd^{2+} is a serious problem during preparation of Cu_2S/CdS multilayered thin films. This issue was addressed by employing polyelectrolyte multilayers on the CdS surface, which completely prevented CdS corrosion, thereby allowing fabrication of heterostructured Cu_2S/CdS films. The formation of polyelectrolyte multilayers is monitored using cyclic voltammetry. The heterostructured films are characterized by structure and morphology. We further employed these films as modified p-channel, p-Cu_2S/n-CdS thin-film phototransistors, where n-CdS acts as the electron transporting and hole-blocking layer that extracts and grounds the photogenerated electrons. This device exhibited a significant increase in photocurrent density (>75 times), drift mobility (>87 times), and good linearity without having to apply gate voltage, when compared to its individual component device.

Introduction

Nanostructured thin-film phototransistors are transistors in which the incident light intensity can modulate charge-carrier density in the channel. Compared with conventional photodiodes, phototransistors enable easier control of light-detection sensitivity without problems such as incremental noise. Scientific and technological advances in solid-state electronics should be achievable with facile fabrication and tailoring of solution-based semiconducting thin films.[1–5,8] Thus, exploring and fabricating high-performance semiconductor thin films in various configurations using the wet chemical route as an economic alternative (in terms of cost, reliability, availability, processability, driving energy, *etc.*),[1–9] and employing these films in novel devices, is a great challenge in contemporary scientific endeavours. Among the solution-processed thin-film transistors (TFTs), organic TFTs have generated great interest because of their potential as a low-cost and light-weight alternative,[1,4,8] but their intrinsic physicochemical and optoelectronic properties determine their application scope. Earlier studies have demonstrated the significance of metal oxide semiconductors (ZnO, SnO_2, In_2O_3, *etc.*) and carbon nanotubes in fabricating photo- and electro-chemically stable TFTs,[2,10,11] which were developed to replace conventional silicon (polycrystalline and amorphous)-based TFTs by overcoming their limitations such as low mobility, non-transparency, and high processing temperatures.[2,10] New semiconductors, chalcogenides[3] and heterojunctions (junction field-effect transistors)[8] are also being explored as viable alternatives to metal oxide semiconductors to overcome issues of gate leakage current and charge transfer efficiency. Chalcogenides semiconductors, with the advantage of unique optoelectronic properties, higher mobility, ready availability, processability, and low cost, have gained acceptance over organic and conventional semiconductors in scientific and technological applications.[9] Although great progress in synthesizing different morphologies and bulk heterojunctions of II–VI (CdS, Cu_2S, CdSe, CdTe, *etc.*) chalcogenides has been achieved,[12] gas-phase deposition techniques have been the methods of choice for a long time, despite the drawbacks of limited precursor materials and use of high-cost vacuum facilities. As alternative approaches, several wet chemical routes have been developed, such as chemical bath deposition (CBD), layer by layer (LbL) deposition, electrodeposition, sol–gel, and spin coating.[3,8,9,13] Recently, Mitzi *et al.*[3] demonstrated an innovative approach for spin coating ultrathin (~50 A°) crystalline semiconducting $SnS_{2-x}Se_x$ films and their application in field-effect transistors. However, LbL deposition of II–VI and III–VI bilayers of semiconductors by the wet chemical route poses a major problem in controlling ion exchange with the metal oxide and

[a]Thin Film and Nanotechnology Laboratory, Department of Physics, Dr Babasaheb Ambedkar Marathwada University, Aurangabad 431004, India. E-mail: rps.phy@gmail.com; Tel: +91-9422-7931-73

[b]Inorganic-Nanomaterials Laboratory, Department of Chemistry, Hanyang University, Sungdong-Ku, Haengdang-dong 17, Seoul 133-791, South Korea. E-mail: shhan@hanyang.ac.kr; Fax: +822-2299-0762

[c]Department of Applied Chemistry, Tianjin University of Technology, Tianjin 300384, People's Republic of China

† Electronic supplementary information (ESI) available. See DOI: 10.1039/c4tc01428f

‡ These authors contributed equally to this work.

chalcogenide surfaces,[14–17] when the first layer is immersed in the precursor solution for depositing subsequent layers.[8] Hence, fabricating multilayer thin films and heterojunctions while addressing the issue of possible ion exchange continues to be a great challenge. Polyelectrolyte multilayers have been used as nanostructure materials;[7] we report the application of the same in fabricating multilayered, chalcogenide thin-film structures *via* a novel approach—controlling and/or prohibiting ion transport through the engineering of cations–anions of polyelectrolyte layers. Although the p-Cu_2S/n-CdS system has been extensively investigated as a solar-cell material with delay times of 60–80 s and has been revisited recently,[18] its application in fabricating thin-film phototransistors (TFPTs) is yet to be explored. TFPTs, which integrate optoelectronic properties combining light detection and signal magnification that realizes great functionality in a single device, are also explored due to their technological advantages over TFTs and photodiodes. The present study reports a new highly stable TFPT device design of a Cu_2S/CdS heterojunction on the indium-tin-oxide (ITO) substrates, successfully fabricated with the aid of protective polyelectrolyte multilayers using a modified wet chemical method. This device is found to exhibit higher photocurrent density than its individual component device.

Experimental

Thin-film deposition

Aqueous solutions of $CdCl_2 \cdot 2H_2O$ (0.02 M, 25 mL) and NH_2CSNH_2 (0.03 M, 25 mL) were prepared separately in deionized (DI) water. The two solutions were mixed in a beaker and stirred constantly with pH maintained at ~11 by adding (2 mL min^{-1}) 27% aq. NH_4OH solution. CdS thin films were deposited using CBD on precleaned ITO substrates, and immersed in the solution for 1 h with reaction bath temperature maintained at 80 °C. The dark yellow-coloured CdS thin films were annealed at 150 °C in air for 1 h. Alternate layers of polyelectrolytes PEI (0.2 g in 100 mL) and PAA (0.2 g in 100 mL) as multilayers, denoted as $(PEI–PAA)_n$ ($n = 0.5, 1.5, 2.5, 3.5$), were dip-coated on the ITO/CdS film at pH ~11 with 1 h of dipping time for each layer. Cu_2S films on ITO and as a subsequent layer on ITO/CdS/$(PEI–PAA)_{1.5}$ substrate were deposited using CBD with a reaction time of 1 h; separately prepared aqueous solutions of $CuSO_4 \cdot 5H_2O$ (0.02 M, 50 mL), triethanolamine (TEA, 0.2 g in 50 mL) and NH_2CSNH_2 (0.02 M, 50 mL) were mixed in a beaker and stirred constantly with pH maintained at 11. The reaction bath temperature was maintained at 40 °C. TEA forms a Cu-metal complex and controls metal oxidation and ion deposition rate. The reaction between Cu^+ and S^{2-} ions forming Cu_2S is confirmed upon observing colour change in the solution from blue to dark brown (10 min) and then golden brown (transparent) after 1 h. The films were washed with DI water, annealed in air at 200 °C (1 h) and subjected to further characterization.

Characterizations

The annealed samples were characterized by powder X-ray diffractometer (XRD, Siemens D-5005, Cu-Kα1 radiation, $V = 40$ kV and I = 100 mA), SEM (Hitachi S-4200), XPS (VG Multi Lab ESCA 2000 system), UV-Vis spectrometer (Cary 100, Japan), and photoluminescence spectrometer (photon-counting spectrometer, ISS Inc.). Current density–voltage (*J–V*) characteristics of the fabricated TFPT devices were obtained in the dark and by varying light intensity (10–100 mW cm^{-2}) using Thermo Oriel Instruments equipment. The ion-permeability study was performed using cyclic voltammetry (CV) with anionic $Fe(CN)_6^{3-}$ and cationic $Ru(NH_3)_6^{3+}$ redox probe molecules.[20] The sandwich layers $(PEI–PAA)_{1.5}$ of the p-Cu_2S/n-CdS thin films annealed at 200 °C (1 h) in air were analyzed using cation and anion spectrums of TOF-SIMS spectroscopy in the imaging modes analysis by conventional methods. The optical image of p-Cu_2S/n-CdS TFPT was obtained *via* conventional methods, when light (source light intensity 100 mW cm^{-2}) allowed in between the source and drain (5 mm × 5 mm) of the device.

Results and discussion

Modifying the electrodes with polyelectrolyte (cations–anions) developed charges on their surface through coulombic interactions with ions in solution, which prohibited ion-exchange reactions and thus protecting the chalcogenide semiconducting films from corrosion/dissolution.[19] Continuing this strategy, alternate layers of polyelectrolyte (PEI and PAA) were employed as ion protecting layers over predeposited CdS layer with the intention of prohibiting Cu^+ ion exchange reactions during subsequent growth of the Cu_2S layer using alkaline CBD. *PEI and PAA have positive and negative ions*, which play important roles such as in the positively charged PEI layers preventing movement of positively charged Cu^+ ions from the solution and attracting negatively charged S^{2-} ions in solution. On the other hand, the PAA layers stacked with PEI layers to form a compact multilayer structure. Consequently, Cu^+ ions in solution could not physically bypass the compact PEI–PAA layers. Thus the Cu^+ ions in solution were unable to reach the CdS surface through the PEI and PAA multilayers or sandwich layers. A cyclic voltammetry (CV) study monitoring ion permeability (which is controlled by surface charge density, that is, quantity of NH_3^+ groups) was used to optimize the pH at ~11 (ESI† Fig. S1a) and the number of polyelectrolyte layers (Fig. 1a) to be employed.[7,20] Fig. 1a shows reduced redox current of the cationic probe with the increasing number of ion-protective $(PEI–PAA)_n$ ($n = 0.5$, 1.5, 2.5, 3.5 as number of bilayers, where $(PEI–PAA)_{0.5}$ means a single PEI layer and $(PEI–PAA)_{1.5}$ means PEI–PAA–PEI alternative layers and so on) layers on the ITO/CdS films with the pH maintained at ~11. Successive shift and decrease in redox current density in the cyclic voltammogram implied effective blocking of cation diffusion with $(PEI–PAA)_n$ (n is 1.5 and above; (see inset, Fig. 1a)). Thus, $(PEI–PAA)_{1.5}$ sandwich layers are used in fabricating highly stable Cu_2S/CdS thin-film heterojunctions and such sandwich layers are converted into cation–anion layers after air annealing at 200 °C for 1 h. In the sandwich layers, the surface charge and structure of polyelectrolyte multilayers are the critical factors to control ion permeability (protection), including after annealing of the thin-film

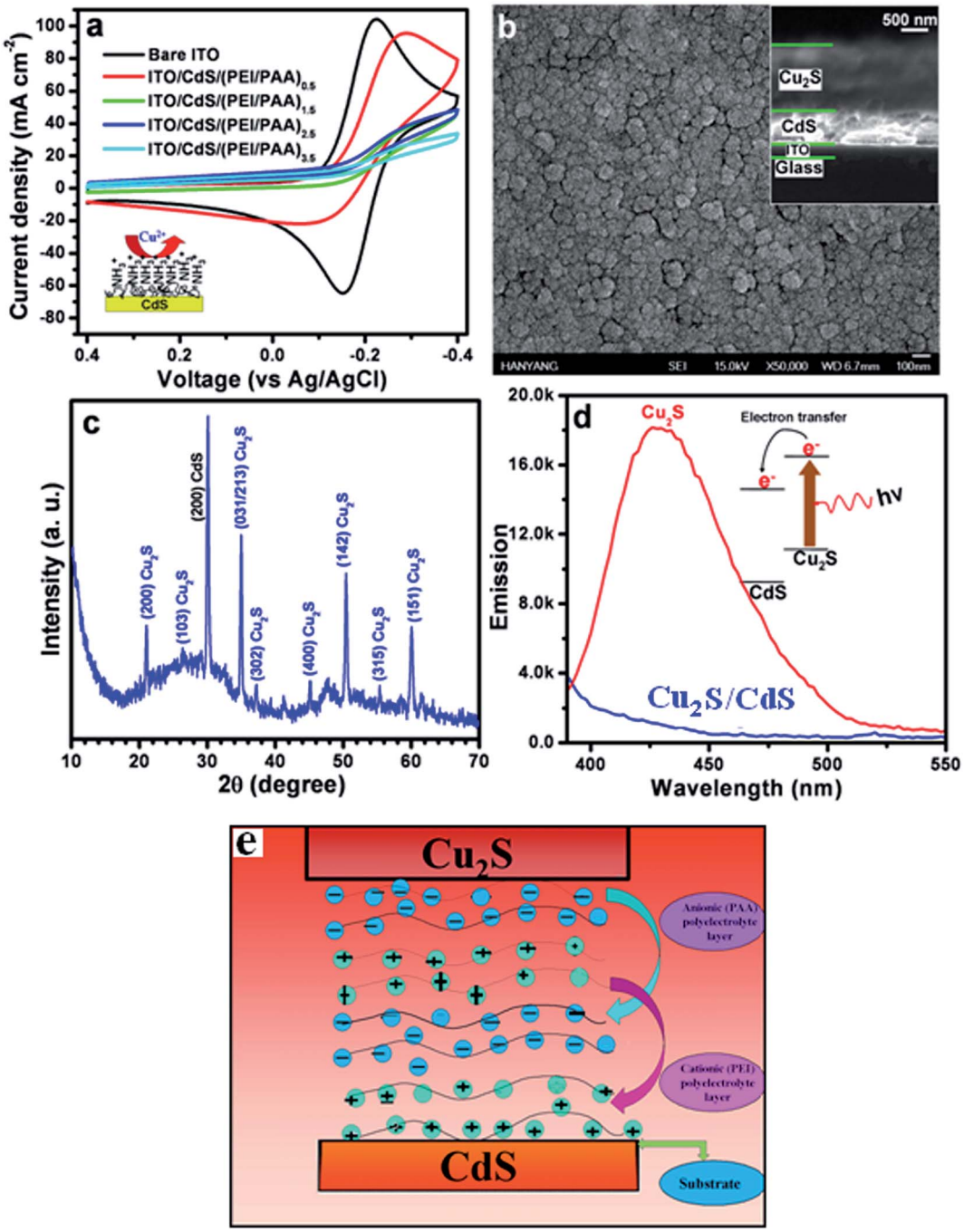

Fig. 1 (a) Cyclic voltammograms obtained using ITO/CdS/(PEI–PAA)$_n$ (n = 0.5, 1.5, 2.5, 3.5) layers and at a fixed pH ~11 to optimize the best condition for blocking Cu^+ cations during the Cu_2S deposition. (b) SEM images obtained from Cu_2S/CdS thin film after annealing. Inset is SEM cross-section view of the film showing CdS and Cu_2S film thicknesses. (c) XRD pattern of the Cu_2S/CdS thin film; the reflection indices are shown in parentheses. (d) Photoluminescence (PL) spectra obtained from Cu_2S/CdS thin film in comparison with Cu_2S film. Inset is the schematic of observed PL quenching. (e) A cartoon image showing the CdS, polyelectrolytes and Cu_2S layers. Polyelectrolytes help to prevent the Cu^+ exchange reaction.

heterojunction (confirmed by time-of-flight secondary ion mass spectrometry [TOF-SIMS] study; see ESI† Fig. S1b and S1c).

The scanning electron microscopy (SEM) image (Fig. 1b) of the Cu_2S/CdS thin film shows a smooth surface with Cu_2S nanoparticles covering the entire CdS layer. The SEM cross-section view of the film shows two distinct layers clearly indicating thicknesses of CdS (~500 nm) and Cu_2S (~1000 nm) films (Fig. 1b inset). Film composition is confirmed from the energy-dispersive X-ray analysis (ESI,† Fig. S2). Quantitative elemental analysis shows the presence of elements in atomic percentages: Cd (25.5%), Cu (28.5%) and S (46.0%). The XRD (Fig. 1c) shows the presence of CdS (cubic phase, PDF 75-1546)

and Cu_2S (orthorhombic phase, PDF-72-0617) structures. This justifies the composition of the Cu_2S/CdS thin-film heterojunction, which is further supported by X-ray photoelectron spectroscopy (XPS) (ESI† Fig. S3). UV-Vis (ESI† Fig. S4) and photoluminescence (PL) spectra (Fig. 1d) were recorded from Cu_2S/CdS thin-film heterojunction and Cu_2S film to study the optical properties and the contribution from Cu_2S film. Higher UV absorption in the 400–700 nm wavelength range, observed as a result of Cu_2S/CdS heterojunction formed at the interface, confirmed that it was not a mere summation of absorption from individual Cu_2S and CdS films. The PL spectrum obtained from the Cu_2S film showed strong emission around 425 nm (Fig. 1d). In contrast, significant PL quenching by a factor of ~50 times was observed from the Cu_2S/CdS thin-film heterojunction as a result of excited-state interactions between CdS and Cu_2S. The observed quenching represents deactivation of the excited Cu_2S *via* energetically favoured electron transfer to the CdS, as it had a lower conduction band (see schematic, Fig. 1d inset).[21] The cartoon image of CdS–polyelectrolyte–Cu_2S layers is shown in Fig. 1e for purposes of enhancing clarity and understanding.

TFPT devices were fabricated using gold metal contacts separated by 5 mm on the thin-film surfaces (Cu_2S/CdS and Cu_2S) that functioned as both source and drain. The photo-illuminated area between the source and drain was assumed to be the virtual gate[22] with ITO grounded in the system. The schematic of the fabricated p-Cu_2S/n-CdS TFPT device (device 1) design is shown in the Fig. 2a inset. The *J*–*V* measurements in the dark and with varying light intensities (10–100 mW cm^{-2}) obtained from device 1 show a significant increase in photocurrent density (Fig. 2a) when compared to the dark, and the individual Cu_2S TFPT device (device 2) (details in ESI†). The dark current densities (0 mW cm^{-2}) in device 1 and device 2 were 8.5 and 0.51 mA cm^{-2}, respectively. Device 1 showed significantly higher photocurrent density (106.5 mA cm^{-2}) when compared to device 2 (1.43 mA cm^{-2}) with 100 mW cm^{-2} light intensity at source voltage of 3.5 V, indicating a nearly 75-fold increase in photocurrent density by adding the n-type layer in the device 1 structure. The observed photocurrent density is higher than reported for most organic TFPTs, metal oxide TFPTs, and chalcogenide-semiconductor-based TFPTs and others in this category.[4,8,13,23] This increased density was attributed to the modified TPFT device design, which effectively separates the photo-generated charge carriers across the p–n junction *via* blocking the holes and simultaneously transferring and grounding electrons through the CdS layer. In turn, the hole concentration was increased and hole transport facilitated in the p-Cu_2S channel by minimizing the possible hole–electron recombination. The process involved (a) generation of excitons *via* the absorption of light; (b) breaking excitons to electrons and holes followed by electron transfer to ground through CdS; and (c) the flow of mobile carriers (holes in this case) in the p-channel Cu_2S layer of the phototransistor *via* the source–drain bias. From Fig. 2a, it is also observed that the saturation in photocurrent density was achieved at levels as low as 3.5 V, which is important from the perspective of device application and technology.

The plot of photocurrent density as a function of light intensity obtained from device 1 shows good linearity in the 0–100 mW cm^{-2} range as compared to low photocurrent density and poor linearity (Fig. 2b and inset with schematic) observed in device 2 of the Cu_2S-only system. Our results imply that the light illumination area in between the source and drain acting as a generated small-area virtual gate controls photocurrent density and device operation. The generated small-area virtual gate was (about 100 × 100 μm^2) measured from the light-activated area, which is confirmed by the optical image photograph, when light is allowed to fall in between the source and drain of the TFPTs devices (ESI†, Fig. 11b). The drift mobility μ, which is a function of carrier concentration, is defined as the velocity v of the charge carriers divided by the electric field E:[23]

$$\mu = \frac{v}{E}, \quad \text{where } v = \frac{I_{DS}}{WQ}, \quad E = \frac{V_{DS}}{L} \tag{1}$$

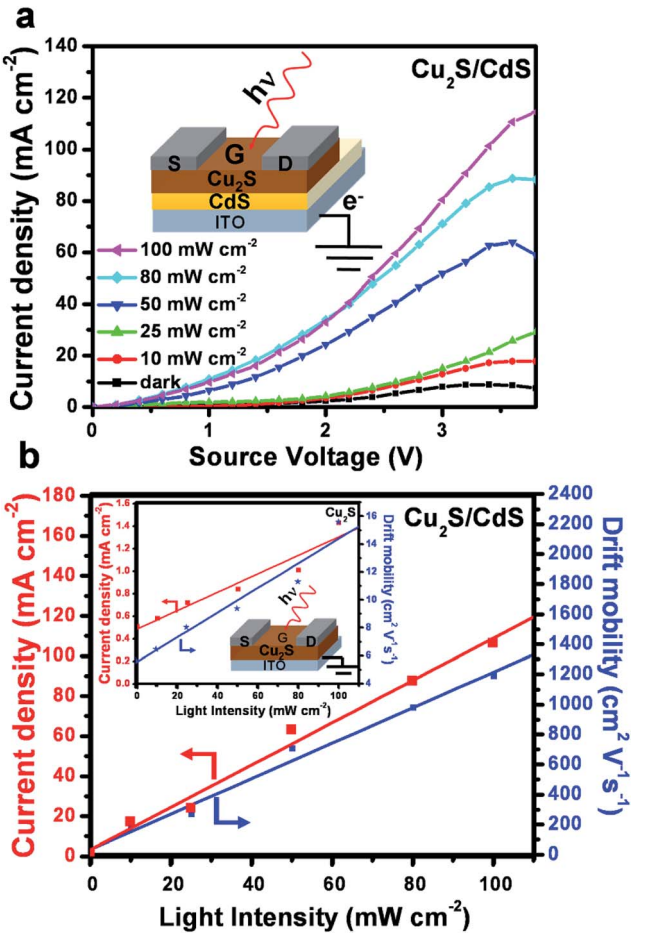

Fig. 2 (a) *J*–*V* plots in dark and with varying light intensities (10–100 mW cm^{-2}) obtained from p-Cu_2S/n-CdS TFPT device showing increase in photocurrent density as a function of light intensity. Inset shows the schematic of p-Cu_2S/n-CdS TFPT device design. (b) Plot of photocurrent density (left *y*-axis scale) and drift mobility μ (right *y*-axis scale) calculated from *J*–*V* data at source voltage of 3.5 V as a function of light intensity (0–100 mW cm^{-2}) obtained from p-Cu_2S/n-CdS TFPT device showing good linearity. Inset shows plot of photocurrent density (left *y*-axis scale) and drift mobility μ (right *y*-axis scale) extracted from *J*–*V* data at source voltage of 3.5 V as a function of light intensity obtained from Cu_2S TFPT device, along with the schematic of the device design.

I_{DS} is the photocurrent obtained at specific source voltage V_{DS} (3.5 V in this case), Q is induced charge per channel area, W (width, 5 mm), and L (length 5 mm) of the TFPT channel. Plot calculations of drift mobility μ as a function of light intensity (0–100 mW cm^{-2}), derived from J–V data for devices 1 and 2, are presented in Fig. 2b and inset. Good linearity in drift mobility was noted for device 1 (Fig. 2b) when compared to device 2 (Fig. 2b inset). It is interesting to note that the drift mobility at the dark current in device 1 (36.2 cm^2 V^{-1} s^{-1}) was ~8 times higher than in device 2 (4.6 cm^2 V^{-1} s^{-1}) and it increased on photoillumination with light intensity (100 mW cm^{-2}) to 1190 and 15.6 cm^2 V^{-1} s^{-1}, respectively, which is ~76 times higher than in device 2 (Cu_2S-only TFPT). This was attributed to the synergistically enhanced hole concentration by effectively draining electrons through the grounded n-CdS layer and at the same time minimizing the hole–electron recombination, creating the observed increase in photocurrent density,[21,23] when compared to its individual component device (Cu_2S only TFPT) and ungrounded n-CdS layer system (details in ESI†).

Conclusions

In summary, we have demonstrated p-Cu_2S/n-CdS heterojunction thin-films in ambient atmospheric conditions using a simple chemical bath deposition (CBD) technique, where polyethyleneimine (PEI) and polyacrylic acid (PAA) play a crucial role as protecting layers. Polyelectrolyte multilayers block Cu^+ ion diffusion, making it possible to deposit Cu_2S on the CdS layer without exchanging Cd^{2+} ions, thereby avoiding damage to the CdS layer during the CBD process. The p-Cu_2S/n-CdS thin-film heterojunction presents valuable structural and chemical properties, excellent optical properties, and J–V characteristics essential for the fabrication of simple and economic phototransistors working in visible light. Further, we fabricated a novel modified p-channel p-Cu_2S/n-CdS TFPT. The significance of the present work lies in the TFPT device design, a unique structure in which n-CdS as the electron-transporting and hole-blocking layer extracts and grounds the photogenerated electrons, minimizing carrier traps or charge recombination in the p-Cu_2S channel and thereby increasing its hole concentration and mobility. This device exhibits a significant increase in photocurrent density (>75 times), drift mobility (>87 times), and good linearity without having to apply gate voltage, when compared to its individual component device, which is attributed to the modified design of p-Cu_2S/n-CdS heterojunction TFPT. From a practical point of view, the modified p–n junction TFPT device was designed for the first time *via* a low-cost wet chemical method using protective polyelectrolyte multilayers and is expected to stimulate further experimental and theoretical investigations along these lines. This approach will become a powerful strategy for fabricating ordered inorganic heterostructured thin-films, with different but selective chemical compositions using the wet chemical route, which are otherwise difficult to grow. We anticipate that our novel p–n junction-based TFPT design with improved performance will be the starting point for new genera of TFPT, TFT, and solar cells. Further improvements in device design, different chemical compositions and techniques in fabricating thin-film phototransistors are underway$ $.

Acknowledgements

This work was supported by the Nano R&D program, Korea Science and Engineering Foundation, South Korean Ministry of Education, Science and Technology (M1080300131008M 030031010) and Brain Korea 21. R.S. grateful for the Brain Pool Fellowship and visiting professorship at Hanyang University (South Korea), and to Dr B.A.M. University, Aurangabad, India, for study leave.

Notes and references

1 (*a*) S. R. Forrest, *Nature*, 2004, **428**, 911; (*b*) C. R. Kagan, D. B. Mitzi and C. D. Dimitrakopoulos, *Science*, 1999, **286**, 945; (*c*) H. E. Katz, A. J. Lovinger, J. Johnson, C. Kloc, T. Siegrist, W. Li, Y. Y. Lin and A. Dodabalapur, *Nature*, 2000, **404**, 478.
2 J. F. Wager, *Science*, 2003, **300**, 1245.
3 D. B. Mitzi, L. L. Kosbar, C. E. Murray, M. Copel and A. Afzali, *Nature*, 2004, **428**, 299.
4 C. D. Dimitrakopoulos and P. R. L. Malenfant, *Adv. Mater.*, 2002, **14**, 99.
5 (*a*) I. Gur, N. A. Fromer, M. L. Geier and A. P. Alivisatos, *Science*, 2005, **310**, 462; (*b*) M. A. Green, K. Emery, Y. Hishikawa and W. Warta, *Prog. Photovoltaics. Res. Appl.*, 2009, **17**, 85.
6 T. Kyratsi, K. Chrissafis, J. Wachter, K. M. Paraskevopoulos and M. G. Kanatzidis, *Adv. Mater.*, 2003, **15**, 1428.
7 X. Shi, M. Shen and H. Möhwald, *Prog. Polym. Sci.*, 2004, **29**, 987.
8 (*a*) S. Cho, J. Yuen, J. Y. Kim, K. Lee, A. J. Heeger and S. Lee, *Appl. Phys. Lett.*, 2008, **92**, 063505; (*b*) X. Liu, Y. Guo, Y. Ma, H. Chen, Z. Mao, H. Wang, G. Yu and Y. Liu, *Adv. Mater.*, 2014, **26**, 3631.
9 R. S. Mane and C. D. Lokhande, *Mater. Chem. Phys.*, 2000, **65**, 1.
10 S. Y. Ju, A. Facchetti, Y. Xuan, J. Liu, F. Ishikawa, P. D. Ye, C. W. Zhou, T. J. Marks and D. B. Janes, *Nature Nanotechnol.*, 2007, **2**, 378.
11 (*a*) S. Kim, S. Ju, J. H. Back, Y. Xuan, P. D. Ye, M. Shim, D. B. Janes and S. Mohammadi, *Adv. Mater.*, 2009, **21**, 564; (*b*) S. E. Ahn, I. Song, S. Jeon, Y. W. Jeon, Y. Kim, C. Kim, B. Ryu, J. H. Lee, A. Nathan, S. Lee, G. T. Kim and U. I. Chung, *Adv. Mater.*, 2012, **24**, 2631–2636; (*c*) S. E. Ahn, S. Jeon, Y. W. Jeon, C. Kim, M. J. Lee, C. W. Lee, J. Park, I. Song, A. Nathan, S. Lee and U. I. Chung, *Adv. Mater.*, 2013, **25**, 5549–5554.
12 (*a*) S. Kumar and T. Nann, *Small*, 2006, **2**, 316; (*b*) W. T. Yao and S. H. Yu, *Adv. Funct. Mater.*, 2008, **18**, 3357; (*c*) X. Wang, J. Zhuang, Q. Peng and Y. D. Li, *Nature*, 2005, **437**, 121; (*d*) D. V. Talapin, J. H. Nelson, E. V. Shevchenko, S. Aloni, B. Sadtler and A. P. Alivisatos, *Nano Lett.*, 2007, **7**, 2951.
13 F. Y. Gan and I. Shih, *IEEE Trans. Electron Devices*, 2002, **49**, 15.
14 J. E. Lilienfeld, in US patent 1745175, USA, 1926.

15 F. Pfisterer, *Thin Solid Films*, 2003, **431**, 470.
16 K. W. Boer, *Phys. Rev. B: Solid State*, 1976, **13**, 5373.
17 A. M. Aldhafiri, G. J. Russell and J. Woods, *Semicond. Sci. Technol.*, 1992, **7**, 1052.
18 Y. Wu, C. Wadia, W. L. Ma, B. Sadtler and A. P. Alivisatos, *Nano Lett.*, 2008, **8**, 2551.
19 Y. Kim, G. Cai, W. Lee, K. Hyung, B. W. Cho, J. K. Lee and S. H. Han, *Curr. Appl. Phys.*, 2009, **9**, S65.
20 M. K. Park, S. X. Deng and R. C. Advincula, *J. Am. Chem. Soc.*, 2004, **126**, 13723.
21 (*a*) P. V. Kamat, *J. Phys. Chem. C*, 2008, **112**, 18737; (*b*) K. Rajeshwar, N. R. de Tacconi and C. R. Chenthamarakshan, *Chem. Mater.*, 2001, **13**, 2765.
22 K. Lee, K. T. Kim, K. H. Lee, G. Lee, M. S. Oh, J. M. Choi, S. Im, S. Jang and E. Kim, *Appl. Phys. Lett.*, 2008, **93**, 193514.
23 K. Ryu, I. Kymissis, V. Bulovic and C. G. Sodini, *IEEE Electron Device Lett.*, 2005, **26**, 716.